



Mixed-mode model for ferrite-to-austenite phase transformation in dual-phase steel



Mélanie Ollat^{a,c}, Matthias Militzer^b, Véronique Massardier^a, Damien Fabregue^a, Eric Buscarlet^c, Fanny Keovilay^c, Michel Perez^{a,*}

^a Univ. Lyon – INSA Lyon – MATEIS – UMR CNRS 5510, F69621 Villeurbanne, France

^b The Centre for Metallurgical Process Engineering, The University of British Columbia, Vancouver, BC V6T 1Z4, Canada

^c Fives Keods, 108-112 Avenue de la liberté, 94700 Maisons-Alfort, FR

ARTICLE INFO

Article history:

Received 28 November 2017

Received in revised form 23 February 2018

Accepted 24 February 2018

Available online 24 March 2018

Keywords:

Dual-phase steels

Intercritical annealing

Austenite formation

Local equilibrium with negligible

partitioning

Mixed-mode model

ABSTRACT

A mixed-mode model is proposed to predict the austenite formation during intercritical annealing of a low-carbon steel with ferrite-cementite microstructure. The transformation kinetics is described by carbon diffusion in combination with an interface mobility, representative of complex phenomena slowing down the transformation rate (solute drag, slow diffusivity of other alloying elements, cementite dissolution). The model approach is formulated to be relevant for complex chemistries typical of industrial steels. Model predictions have been successfully benchmarked with experimental data including heating and holding stages at various heating rates and holding temperatures.

Crown Copyright © 2018 Published by Elsevier B.V. All rights reserved.

1. Introduction

The significant increase of the use of Advanced High-Strength Steels (AHSS) has greatly intensified the number of studies focused on their microstructure evolution during processing, where complex thermo-mechanical treatments are performed. In particular, the austenite-to-ferrite transformation has been widely investigated occurring during cooling [1]. Less attention was paid to the ferrite-to-austenite transformation taking place during heating. There are a number of challenges to study the formation of austenite including: (i) the large number of possible structures on which austenite forms [2–4]; (ii) the high-temperature at which austenite forms; (iii) the austenite decomposition during cooling makes it difficult to follow its formation. However, in order to optimize the heating and holding stages in an industrial production line, e.g. hot dip galvanizing line, it is important to predict the evolution of the austenite phase fraction as a function of time/temperature. Thus, a simple yet physically motivated model is required for intercritical austenite formation in AHSS.

Abundant literature has been dedicated to the austenite-to-ferrite transformation (see the rather complete review of Gouné et al. [5]). However, models accounting for the ferrite-to-austenite transformation are relatively scarce. Frequently, the Johnson-Mehl-Avrami-Kolmogorov (JMAK) model [6–8] is employed to empirically describe the kinetics [9,10] but lacks physical basis, limiting its predictive capability. From a more fundamental perspective, the austenite formation is usually modeled based on the diffusion of elements controlling the transformation rate. Such diffusion-controlled models are based on the numerical solution of Fick's equation [11,12]. Atkinson et al. [13] modeled the interface motion based on the local equilibrium at the interface for a binary Fe-C system. Wycliffe et al. [14], proposed a simplified diffusive model to account for austenite growth in a ternary Fe-Mn-C system. They successfully compared the experimental and modeled Mn concentration profile during transformation, but did not provide global transformation kinetics. More recently, Lai et al. [15] used DICTRA software to model the formation of austenite from spheroidized cementite lying in a ferrite matrix. This approach led to very satisfactory results but requires complex calculations to track the motion of both cementite/austenite and austenite/ferrite interfaces.

Alternatively, Christian [16] introduced the concept of interface-controlled transformation. Supposing fast (infinite) diffusion, the transformation rate depends on the local driving pressure

* Corresponding author.

E-mail addresses: melanie.ollat@insa-lyon.fr (M. Ollat), matthias.militzer@ubc.ca (M. Militzer), veronique.massardier@insa-lyon.fr (V. Massardier), damien.fabregue@insa-lyon.fr (D. Fabregue), eric.buscarlet@fivesgroup.com (E. Buscarlet), fanny.keovilay@fivesgroup.com (F. Keovilay), michel.perez@insa-lyon.fr (M. Perez).

and the interface mobility. However, in general, neither the interface mobility nor the diffusion are infinite [17]. The transformation has a mixed-mode character, *i.e.* is controlled by both diffusion and interface mobility.

Mixed-mode models were initially developed for the austenite-to-ferrite transformation [18–20]. Supposing non-infinite interface mobility, these authors implemented an algorithm leading to a deviation from local equilibrium at the interface (as otherwise assumed for fully diffusion-controlled models). This deviation generates a driving pressure for the interface motion. Bos et al. [20] applied the mixed-mode model to describe ferrite formation during cooling at different rates of a 0.42C–1.72Mn (wt%) steel with good accuracy. Here the ternary alloy is reduced to a quasi-binary system by obtaining the driving pressure with respect to local equilibrium with negligible partitioning (LENP). Such simplification ensures easier and faster computational calculation but is only possible when Mn diffusion remains negligible (*i.e.* as for cooling treatments).

Mecozzi et al. conducted a comparative study between the diffusion-controlled, interface-controlled and the mixed-mode model for the ferrite-to-austenite transformation [21]. They did however not provide any experimental data to compare with their approaches.

Chen and Van der Zwaag [22] proposed a generalised mixed-mode model based on Gibbs energy balance (GEB) accounting for the diffusion of C and other substitutional element(s). Their model could explain the stasis phenomenon occurring during the austenite-to-ferrite transformation, but has not been applied to the reverse transformation.

Other types of numerical models based on a 2D/3D description of the microstructure have been recently proposed [23–26]. An original Cellular Automaton (CA) approach has been developed by Bos et al. [23]. In this model, the microstructure evolution is described by moving interfaces according to an interface-controlled model. More recently, Zheng and Raabe [25] also proposed such kind of model using mixed-mode growth kinetics coupled with a 2D-diffusion model. Unfortunately, these CA models were not compared with experimental transformation kinetics.

Phase Field (PF) models have been used to describe the 2D evolution of the microstructure during intercritical annealing treatments. Zhu and Militzer [26] proposed a rather complete PF model accounting for: (i) nucleation of austenite; (ii) growth from pearlite and/or ferrite (based on mixed-mode model); (iii) recrystallization of deformed ferrite grains. Although compared successfully with experiments, this approach is costly in computational resources and thus not suitable to control the production of intercritically annealed steel as on-line tool.

This paper proposes a simple yet physically based implementation of the mixed-mode model for the ferrite-to-austenite phase transformation occurring during intercritical annealing treatments, having a DP 1000 steel as an example. The diffusion field is simulated and combined with the prediction of interface motion to calculate the overall kinetics of austenite formation. Results of the model are discussed and compared to experimental transformation kinetics, detailed in a companion paper [10].

2. Mixed-mode model

2.1. Model formulation

When the temperature exceeds Ae_1 (equilibrium austenite start temperature), austenite starts to form with a composition that may be different from the one of the parent phase. The mixed-mode model [18–21] accounts for both C diffusion and the limited mobility of the sharp ferrite/austenite interface due to drag of the Mn

spike [27–28]. In this mixed-mode model, the transformation is hence controlled by both C diffusion and interface mobility.

A schematic representation of the mixed-mode model is given in Fig. 1. Initially, at the Ae_1 temperature and time $t_0 = 0$, a cementite/ferrite equilibrium system is assumed. When the temperature exceeds Ae_1 , austenite becomes thermodynamically stable. At t_0 , it is assumed that cementite immediately transforms into austenite with the same composition (6.7 wt% of C). The initial austenite is therefore carbon supersaturated.

A 1D simulation cell of size z_M is assumed, within which the carbon content in austenite and ferrite phases is modeled according to Fick's equation:

$$\frac{\partial C}{\partial t} = D \frac{\partial C}{\partial z} \quad (1)$$

where C is the carbon concentration and D the diffusion coefficient of carbon. Here, we assume that molar volumes of ferrite and austenite are equal, so that volume concentrations are equal to molar concentrations.

The limited interface velocity may generate carbon accumulation building up at the interface. The deviation from equilibrium induces a driving pressure ΔG to displace the interface into the ferrite phase:

$$\Delta G = \chi(T)(C_C^{\gamma int} - C_C^{\gamma Eq}) \quad (2)$$

where $C_C^{\gamma int}$ and $C_C^{\gamma Eq}$ are the austenite carbon content at the interface and the austenite equilibrium C content, respectively.¹ $\chi(T)$ is a temperature dependent parameter (unit: $J mol^{-1} wt\%^{-1}$) linking the transformation driving pressure ΔG with the deviation of the carbon concentration from equilibrium, $\Delta C = C_C^{\gamma int} - C_C^{\gamma Eq}$.

The interface velocity v is proportional to ΔG via the mobility M of the interface:

$$v = M \Delta G \quad (3)$$

At an intermediate time t , the concentration profile is characterized by a gradient of carbon at the austenite side. The gap between the carbon concentration at the interface and the equilibrium highlights the coupling between diffusion-controlled and interface-controlled models.

The system evolves until equilibrium is reached in terms of phase fraction and carbon composition.

Analog to the $\gamma \rightarrow \alpha$ phase transformation, the degree of the mixed-mode character may be quantified by the mode parameter S [18]. For the reverse $\alpha \rightarrow \gamma$ transformation, the S parameter is expressed by the following equation:

$$S = \frac{C_C^{\gamma int} - C_C^{\gamma Eq}}{C_C^{\gamma \infty} - C_C^{\gamma Eq}} \quad (4)$$

with $C_C^{\gamma int}$, $C_C^{\gamma Eq}$ and $C_C^{\gamma \infty}$ austenite carbon content respectively at the interface, at the thermodynamic equilibrium and far away from the interface (*i.e.* $z_M = 0$). Here $S = 0$ means that the transformation is diffusion-controlled whereas $S = 1$ indicates an interface-controlled mode. The mode parameter is in the range $0 < S < 1$ in the case of mixed-mode transformation. The detailed numerical algorithm used in this work is presented in Appendix A.

¹ Note that equilibrium does not necessarily mean full equilibrium, also called Ortho Equilibrium (OE). As explained in Ref. [31], the transformation can also occur under, Local Equilibrium (LE), Para-Equilibrium (PE), Local Equilibrium with Negligible Partitioning (LENP), *etc.* Discussion on the chosen thermodynamical equilibrium is given in the “model parameters” section.

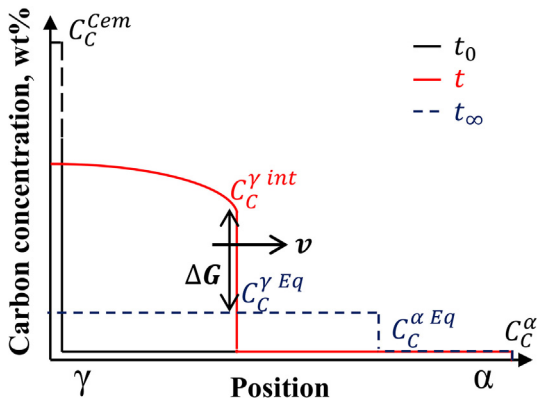


Fig. 1. Schematic representation of the mixed-mode model system. Carbon concentration profiles are plotted at different times: the initial time t_0 , an intermediate time t and the infinite time t_{∞} when the austenite-ferrite equilibrium is reached.

2.2. Materials, initial state and model parameters

The mixed-mode model was applied to describe the austenite formation kinetics during intercritical treatments of a recrystallized 0.17C-1.763Mn-0.427Cr-0.345Si-0.037Al (wt%) steel with a ferrite/cementite initial microstructure. More details on material, techniques and experimental data are given in the previous paper by Ollat et al. [10]. Thermo-Calc software [29] with the TCFE8 database [30] was employed to obtain the required information on the thermodynamics of the ferrite-austenite transformation.

Assuming a flat austenite-ferrite interface one dimensional simulations are carried out where the length of the system is set to $z_M = 2 \mu\text{m}$, which corresponds approximatively to half the ferrite grain size. This assumption implies that nucleation occurs at cementite located at ferrite grain boundaries under the hypothesis of nucleation site saturation as mentioned in Ref. [31], i.e. the nuclei density is a function of ferrite grain size but independent of heating rate.

Initially, the system is defined by the thermodynamic equilibrium state before reaching Ae_1 (685 °C). Hence the two phases, cementite and ferrite, are assumed at the initial time t_0 as schematically shown in Fig. 1. The length of cementite was set to 48 nm replicating its equilibrium fraction (2.44 vol%). The carbon equilibrium concentrations are 6.7 wt% in cementite and 0.005 wt% in ferrite.

Above Ae_1 , cementite is assumed to immediately transform into austenite, in agreement with the fast dissolution of cementite proposed by Gouné et al. [31]. Whereas the carbon chemical potential is constant in both phases (flat concentration profiles), the transformation immediately initiates because these chemical potentials are different: the initial carbon concentration in the austenite (6.7 wt%) is well above its equilibrium value.

Contrary to Mecozzi et al. [21], the thermodynamic equilibrium is considered to occur through Local Equilibrium with Negligible Partitioning (LENP) condition for the $\text{Fe}_3\text{C} + \alpha \rightarrow \gamma$ transformation. While paraequilibrium assumes a constraint equilibrium where only C is at equilibrium, LERP supposes localized Mn redistribution at the interface (Mn spike). The LERP hypothesis is more accurate, as proved experimentally [10]. Note that in the mixed mode model, during the transformation, even C is not truly at equilibrium (due to interface mobility) and thus Bos et al. [20] appropriately called the interface contact condition “Mixed Mode Negligible Partitioning” (MMNP).

The LERP condition provides the final austenite fraction for a given intercritical temperature. The construction of LERP is illus-

trated on the 760 °C-isothermal section of the ternary Fe-C-Mn phase diagram in Fig. 2. The investigated composition is identified by a red star and the orthoequilibrium (ORTHO) tieline passing through this bulk composition is also reported. The local equilibrium (LENP) tieline corresponds to the one for which the Mn composition in the newly formed austenite is equal to the bulk Mn content. The final state of LERP condition is characterized by flat carbon profiles and a Mn spike at the ferrite/austenite interface. The associated carbon composition in ferrite and austenite phases, according to LERP, are given in Fig. 3.

To describe the austenite formation kinetics, the carbon diffusivity is taken from Bhadeshia [32] with diffusion coefficients calculated from: $Q_C^{\alpha} = 80 \text{ kJ/mol}$, $D_{0c}^{\alpha} = 6.2 \times 10^{-7} \text{ m}^2/\text{s}$ for the ferrite; and for the austenite: $Q_C^{\gamma} = 135 \text{ kJ/mol}$, $D_{0c}^{\gamma} = 1.0 \times 10^{-5} \text{ m}^2/\text{s}$. The mobility parameter M is considered as a fit parameter in the present study.

For the interface velocity module, the $\chi(T)$ parameter involved in the driving pressure ΔG is obtained from Thermo-Calc calculations as proposed by Mecozzi et al. [21]. Considering Eq. (2), the Gibbs energy of the austenite G^{γ} as a function of the carbon content C_C^{γ} and temperature is required to determine, $\chi(T)$ which is then derived by plotting $\partial G_C^{\gamma} / \partial C_C^{\gamma}$ as a function of the temperature as shown in Fig. 4 and subsequently approximated by a polynomial function. The mobility parameter M is considered as a fit parameter in the present study.

3. Results and discussion

The mixed-mode model was implemented for complex thermal cycles including heating and holding stages. The heating rate R_H , annealing time and temperature are input parameters of the mixed-mode model.

3.1. Influence of the interface mobility parameter M

Fig. 5 illustrates the influence of the mobility parameter M in the mixed-mode model. The austenite formation kinetics was calculated at 760 °C for three different values of the mobility: (i) $M = 7 \times 10^{-7}$; (ii) $M = 10^{-8}$ and (iii) $M = 10^{-12} \text{ mol m J}^{-1} \text{ s}^{-1}$ as shown in Fig. 5a. The evolution of the mixed-mode degree S with the interface mobility M is plotted in Fig. 5b. In addition, carbon evolution profiles in austenite and ferrite phases are plotted in Figs. 5c, d and e, respectively.

The highest mobility value ($M = 7 \times 10^{-7} \text{ mol m J}^{-1} \text{ s}^{-1}$, represented in blue colour) generates a quick austenite formation (less than 1 s). The associated S parameter is equal to 0 highlighting a diffusion-controlled mode. Interface motion is not restricted so that the kinetics is only controlled by the carbon diffusion and local equilibrium is maintained at the interface as reflected by the equality of the austenite carbon content at the interface $C_C^{\gamma int}$ with the austenite equilibrium value $C_C^{\gamma Eq}$ as shown in Fig. 5c.

On the contrary for the smallest mobility value ($M = 10^{-12} \text{ mol m J}^{-1} \text{ s}^{-1}$, represented in green colour), the phase transformation is considerably delayed to longer holding times. The mode parameter S is equal to 1 meaning an interface-controlled transformation. The corresponding carbon profiles (Fig. 5e) are flat in both phases. The carbon diffusion is thus no longer controlling the kinetics, only the interface reaction drives the phase transformation. The deviation between equilibrium and interface austenite carbon content induces the driving pressure ΔG for interface motion.

An intermediate mobility value ($M = 10^{-8} \text{ mol m J}^{-1} \text{ s}^{-1}$, represented in red colour) leads to a transformation kinetics in between diffusion-controlled and interface-controlled kinetics as expected

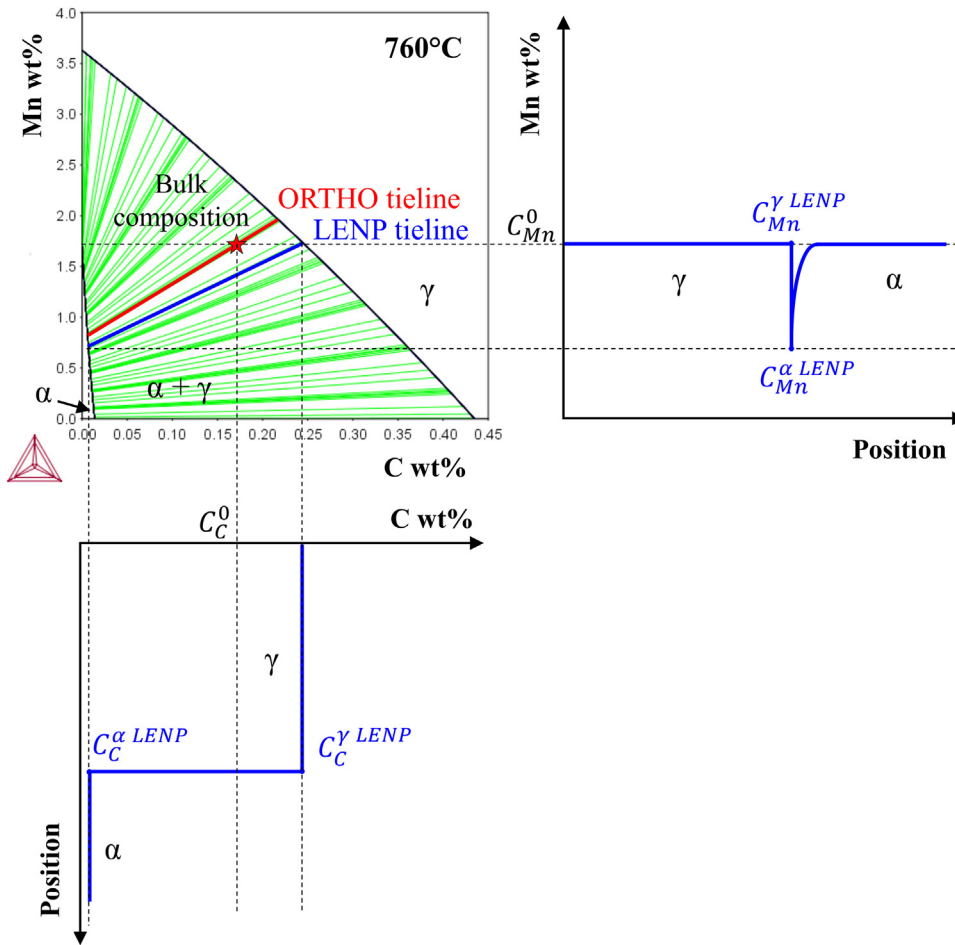


Fig. 2. Isothermal section of the Fe-C-Mn phase diagram at 760 °C (Thermo-Calc). The tieline and concentration profiles according to LENP condition at final time are plotted for the bulk composition Fe-0.17 wt% C-1.763 wt% Mn, marked by a red star.

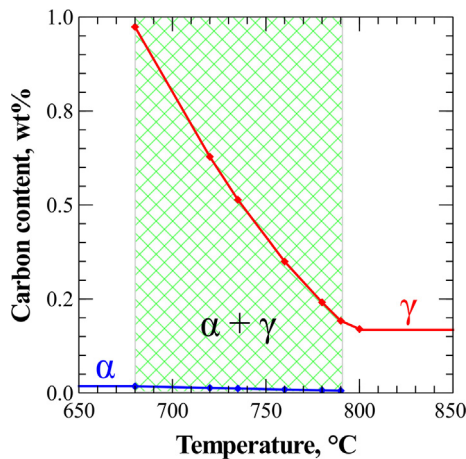


Fig. 3. Carbon contents in α and γ phases for the nominal composition Fe-0.17 wt% C-1.763 wt% Mn as a function of temperature assuming LENP condition (Thermo-Calc).

in the mixed-mode model. The S value is close to 0.5 indicating that both diffusion and interface mobility contribute to the kinetics of phase transformation. The austenite carbon content at the interface decreases with time to reach the equilibrium value (Fig. 5d).

The average mode parameter S is plotted as a function of the interface mobility at 760 °C in Fig. 5b. Below a mobility of 10^{-10}

$\text{mol m}^{-1} \text{s}^{-1}$, the mode parameter S is equal to 1 meaning that the transformation is interface-controlled. For a sufficiently large mobility, i.e. above $7 \times 10^{-7} \text{ mol m}^{-1} \text{s}^{-1}$, the transformation is carbon diffusion controlled. The transformation is thus mixed-mode controlled when the interface mobility is in the range of $10^{-10} < M < 7 \times 10^{-7} \text{ mol m}^{-1} \text{s}^{-1}$.

3.2. Comparison with experiments

The model was applied to describe the phase transformation on typical industrial annealing cycles considering both the heating and holding stages. The mobility parameter is assumed to depend on temperature following a classical Arrhenius behaviour:

$$M = M_0 \exp \left[-\frac{Q_m}{RT} \right] \quad (5)$$

where the apparent activation energy Q_m and the pre-exponential M_0 of the mobility were adjusted with experimental data for heating at $R_H = 5 \text{ °C/s}$ and then holding at 735, 760 and 780 °C, respectively.

Fig. 6a compares the mixed-mode model and experimental austenite fraction during these three heating cycles. The thermal cycles are also added allowing to follow the temperature evolution during the heating step. Please note, the time scale starts when the temperature equals $Ae_1 = 685 \text{ °C}$.

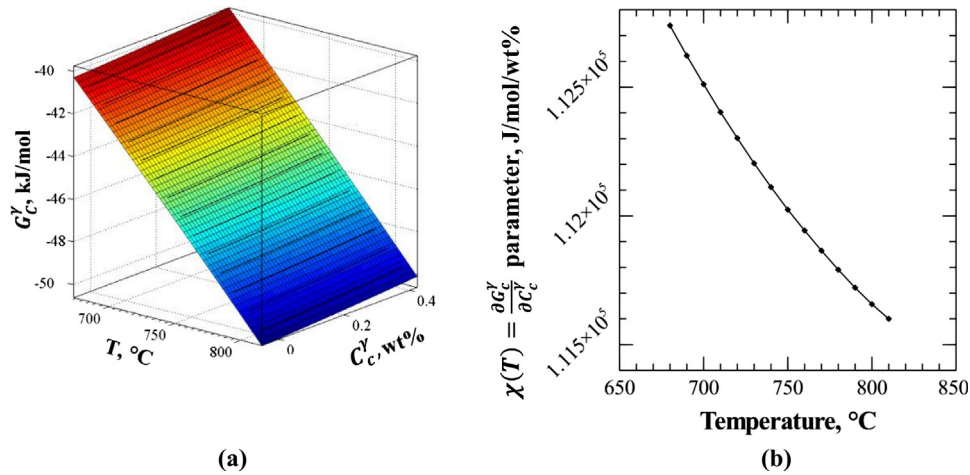


Fig. 4. (a) Gibbs energy of the austenite phase as a function of temperature and carbon content (Thermo-Calc) (b) Representation of $\chi(T)$ as a function of temperature.

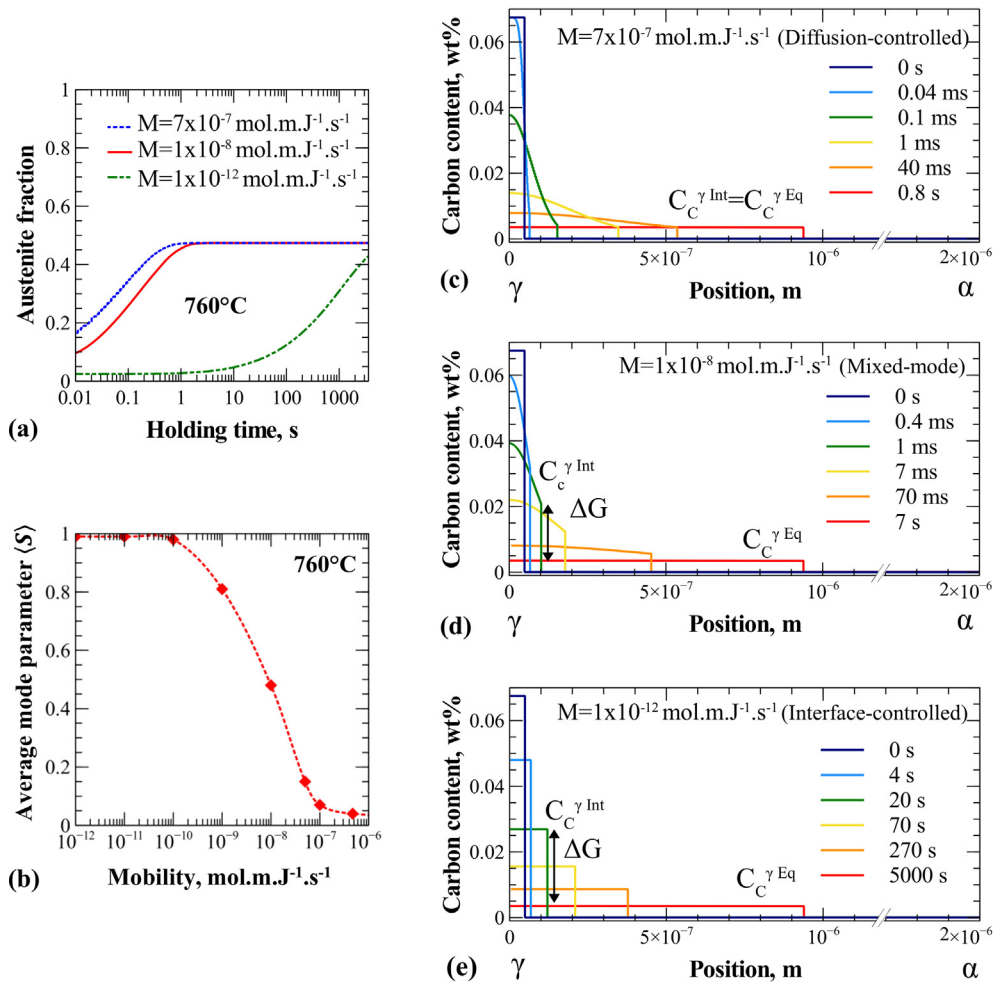


Fig. 5. (a) Kinetics of austenite formation during isothermal holding at 760 °C, for different conditions: carbon diffusion-controlled ($M = 7 \times 10^{-7} \text{ mol m J}^{-1} \text{ s}^{-1}$), mixed-mode ($M = 10^{-8} \text{ mol m J}^{-1} \text{ s}^{-1}$) and interface-controlled ($M = 10^{-12} \text{ mol m J}^{-1} \text{ s}^{-1}$). (b) Evolution of the average mode parameter $\langle S \rangle$ as a function of the interface mobility. (c), (d), (e) Carbon concentration in austenite and ferrite for different holding times and the three interface mobility considered here.

The best description of the three experimental kinetics at 735, 760 and 780 °C is obtained for $Q_m = 900 \text{ kJ/mol}$ and $M_0 = 5 \times 10^{35} \text{ mol m J}^{-1} \text{ s}^{-1}$.

This mobility parameter set was applied for 100 °C/s heating rate ramp plus holding stage as shown in Fig. 6b. The experimental

kinetics are again well predicted using the same mobility parameters as for the 5 °C/s heating rate. Moreover it can be noted that at the higher heating rate, less austenite is formed during the heating stage because there is less time for transformation to occur. This is particularly visible for the highest holding temperature (780 °C)

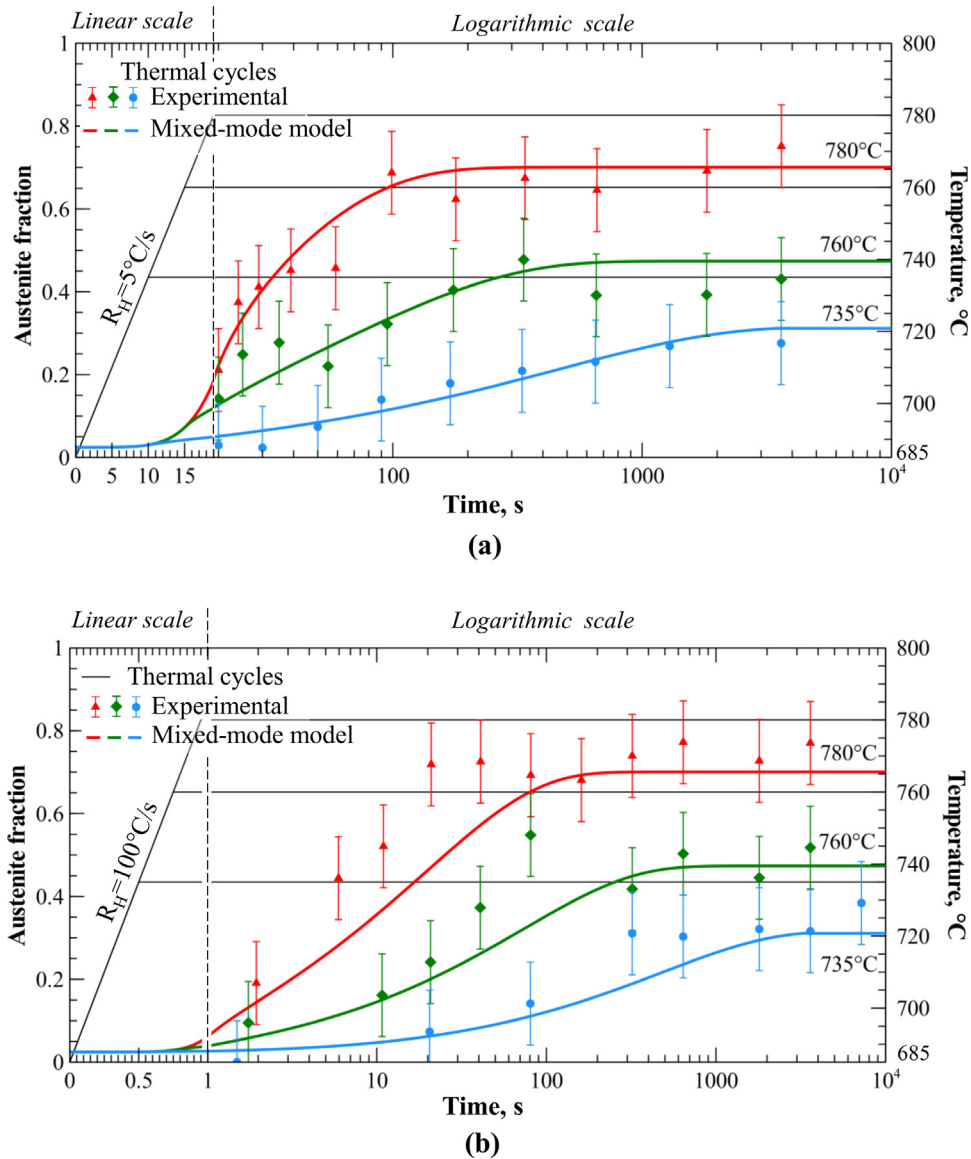


Fig. 6. Experimental and mixed-mode model kinetics for austenite formation during isothermal holding after a heating stage of (a) 5 and (b) 100 °C/s. Mobility parameters are fixed to $Q_m = 900$ kJ/mol and $M_0 = 5 \times 10^{35}$ mol m J⁻¹ s⁻¹.

where 23% of austenite is formed during the heating stage at 5 °C/s against less than 15% at 100 °C/s.

Experimental and model continuous heating transformation kinetics are compared for different heating rates (5, 7.5, 10 and 30 °C/s) in Fig. 7. Mobility parameters are the same as for heating and isothermal holding conditions shown in Fig. 6. The model allows to accurately describe the initial portions of austenite formation up to 80% transformed for the lowest heating rate of 5 °C/s and up to 60% transformed for the highest heating rate of 30 °C/s. The shift of the austenite formation to higher temperature with increasing heating rate is appropriately captured. The discrepancies between model and experimental results for the final transformation stages may be related to the fact that these transformation stages occur at higher temperatures, i.e. above 780 °C, than considered for establishing the mobility parameters. The limitations of extrapolating the interface mobility to these higher temperatures may indicate a significant widening of the Mn spike at the interface due to increased diffusion of Mn. From an industrial perspective,

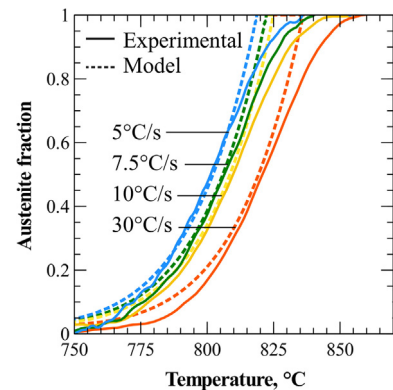


Fig. 7. Experimental and mixed-mode model kinetics for austenite formation during heating treatment with rate of 5, 7.5, 10 and 30 °C/s. Mobility parameters are fixed to $Q_m = 900$ kJ/mol and $M_0 = 5 \times 10^{35}$ mol m J⁻¹ s⁻¹.

however, this limitation is less significant, as intercritical annealing is typically not carried out at these higher temperatures.

3.3. Discussion

The mixed-mode model proposes a fairly good description of the experimental phase transformation kinetics in typical industrial annealing cycles. The same mobility parameters were used to predict the ferrite-to-austenite transformation for all heating rates (5–100 °C/s) and annealing temperatures (735–780 °C). The mobility parameters are $Q_m = 900$ kJ/mol and $M_0 = 5 \times 10^{35}$ mol m J⁻¹ s⁻¹ for the selected steel, such that the mobility varies by more than four orders of magnitude between 700 and 800 °C (see Fig. 8). Note that the proposed activation energy for mobility, Q_m , is very high and can not be associated with any physical event. These parameters provide a convenient description of the friction force applied to the interface. The slowing down of the interface migration rate may be associated with Mn diffusion and segregation across the interface as experimentally observed in the quaternary Fe-C-Mn-Si system by Qui et al. [27].

In the literature, Q_m is however commonly adopted to be 140 kJ/mol (Refs. [19,21,33]) as the typical activation energy for grain-boundary migration. The present Q_m is considerably higher than the one commonly used. However, three remarks can be pointed out: (i) To our knowledge, published mixed-mode model kinetics, validated with experimental data are already scarce for $\gamma \rightarrow \alpha$ transformation [18–20], and inexistent for the reverse $\alpha \rightarrow \gamma$ transformation; (ii) Despite large difference between literature and used activation energy (Q_m), the mobility M lies in a domain [$8 \times 10^{-9} - 2 \times 10^{-13}$] mol m J⁻¹ s⁻¹, comparable with the literature: [$1 \times 10^{-8} - 8 \times 10^{-9}$] mol m J⁻¹ s⁻¹ (Mecozzi et al. [21]), 5×10^{-8} mol m J⁻¹ s⁻¹ (Sietsma et al. [18]), [$1 \times 10^{-9} - 8 \times 10^{-9}$] mol m J⁻¹ s⁻¹ (Bos et al. [19]), [$7 \times 10^{-9} - 3 \times 10^{-8}$] mol m J⁻¹ s⁻¹ (Zhu et al. [34]) for temperatures ranging from 700 to 800 °C; (iii) Activation energy (Q_m) should rather be seen as an *effective* activation energy accounting for several coupled mechanism: cementite dissolution, diffusion of substitutional alloying elements, solute drag etc. Note that Gouné et al. [31] pointed out that cementite dissolution is a first order limiting factor at temperatures ranging from 700 to 740 °C.

For all considered complex thermal cycles, composed of a heating followed by a holding stage (Fig. 7), the mixed-mode parameter

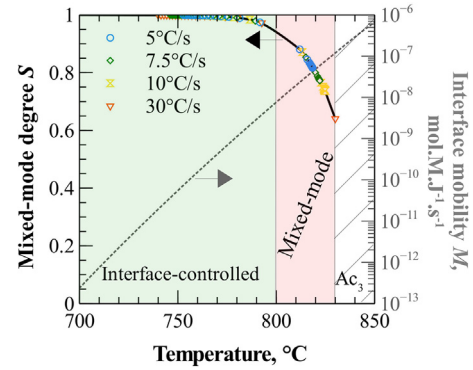


Fig. 8. Mixed-mode degree of the ferrite-to-austenite transformation. At temperatures lower than 800 °C, the transformation kinetics is solely controlled by the interface mobility. At higher temperatures, the transformation exhibits a mixed-mode character, accounting for the diffusion of C and other phenomena (substitutional element diffusion, solute drag).

S is equal to 0.99, which is characteristic of an interface-controlled mode as carbon diffusion is quick compared to all above-mentioned mechanisms responsible for interface mobility. The mode parameter S is however different from 1 in the case of the continuous heating conditions presented in Fig. 7. In Fig. 8, the mixed-mode parameter S is plotted vs temperature for the continuous heating conditions. At temperatures lower than 800 °C, the transformation kinetics is controlled by the interface mobility. At higher temperatures, the proposed transformation model exhibits a mixed-mode character, accounting for the diffusion of C and other phenomena (substitutional element diffusion, solute drag, cementite dissolution). In such conditions, the mobility of the interface becomes fast enough at high temperature to induce a transformation partly controlled by carbon diffusion.

In Fig. 8, it can be seen that all S values superimpose on a unique master curve for all investigated heating rates. The mixed mode character of the transformation appears to be temperature dependent.

The mixed-mode character may be observed in the case of fast heating rates where transformation occurs at higher temperatures. Fig. 9 shows the calculated carbon profile during heating at 30 °C/s to various temperatures ranging from 685 to 835 °C. The curved carbon profile in austenite observed at 800, 825 and 835 °C

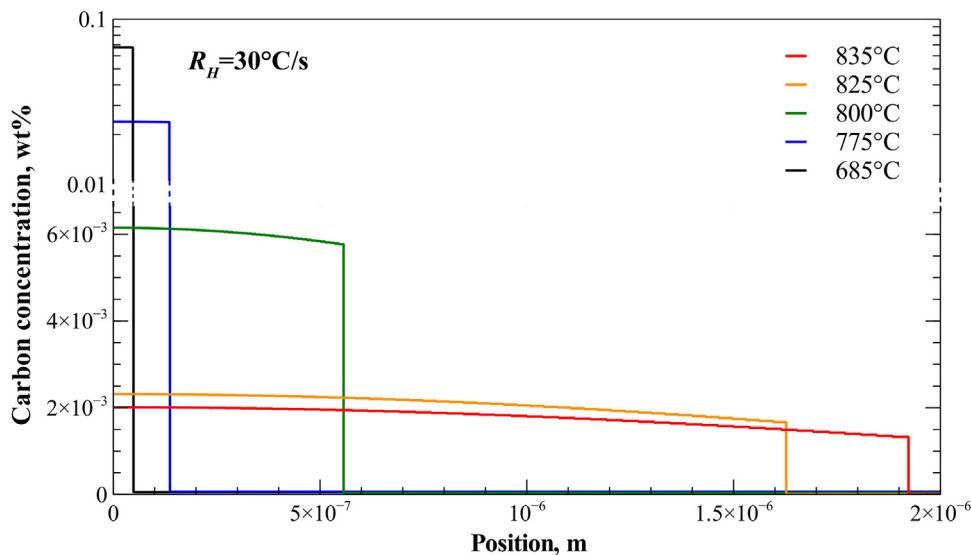


Fig. 9. Evolution of the carbon evolution profile during the heating at 30 °C/s and interrupted at different temperatures in between 685 and 835 °C. Mobility parameters are fixed to: $Q_m = 900$ kJ/mol and $M_0 = 5 \times 10^{35}$ mol m J⁻¹ s⁻¹.

suggests that diffusion also drives interface motion at temperature higher than 800 °C.

Note that equilibrium used to calculate the driving pressure (Eq. (2)) is not ortho-equilibrium, but rather an analog to LENP, where the forming phase has the same Mn composition as the parent phase. This is in accordance with the hypothesis at the basis of the mixed-mode model: (i) only C diffuses; (ii) and other substitutional elements slow down interface migration by solute drag effects but do not experience long range diffusion.

The mixed-mode model requires Q_m and M_0 to be adjusted for any steel chemistry. Due to these simplifying assumptions, the mixed-mode model cannot capture some physical features such as Mn enrichment of cementite that can modify the transformation kinetics [15,35]. With two fitting parameters, it allows to describe a wide range of experimental observations for a given steel chemistry. The model captures with good accuracy the asuttenite formation kinetics for typical intercritical annealing cycles including heating and holding stages.

The mixed-mode model, as presented in this paper can be seen as an intermediate stage between the purely descriptive JMAK approaches and more complex thermodynamical multicomponent diffusion calculations involving transition from LENP to ORTHO equilibrium (e.g. DICTRA [15,35]). The mixed-mode model allows a step towards more fundamental formulations and description of complex systems. An artificial mobility value ensures to account for complex mechanisms induced by the presence of substitutional elements. Such a simplified simulation tool allows to bypass many modeling challenges for multi-component systems including the determination of operative tie-lines, the initial partitioning of substitutional elements, as well as a multi-component solute drag analysis.

Finally, this model provides a reasonable tool for describing austenite formation occurring during heating of DP steels in conditions that are typical of an industrial production line alloy. In practice, for each new steel composition, the parameter M needs to be calibrated using isothermal and/or non-isothermal experiments. Then, the quickness of calculations makes such a tool convenient to control and/or optimize, on-the-fly, the different process parameters of the production line.

4. Conclusions

A mixed-mode model with negligible partitioning is proposed to describe the austenite formation from a ferrite/cementite microstructure in a low carbon steel with a chemistry typically

employed for DP 1000 steels. The transformation kinetics depends on both carbon diffusion and interface mobility. The interface mobility is an effective parameter that mostly accounts for diffusion of slow elements (e.g. Mn), cementite dissolution and/or solute drag effects.

A unique mobility set (Q_m and M_0) was used to model transformation kinetics for a given steel chemistry. Simulation results were successfully compared with experiments for both isothermal and non-isothermal conditions at various heating rates and annealing temperatures.

The model exhibits two transformation modes: below 800 °C, transformation kinetics is controlled by interface mobility; above 800 °C, both interface mobility and C diffusion control the transformation kinetics, providing thus a mixed-mode character to the transformation.

To our knowledge, the mixed-mode model with LENP conditions (analog to $\gamma \rightarrow \alpha$ transformation) has never before been applied to austenite formation. Such a model is relevant to describe the phase transformation for complex chemistries, as generally used in industrial steels.

While the adjustment of mobility parameters is required, the proposed model provides a simple and physically based tool for predicting austenite formation in advanced high strength steels.

Acknowledgements

Authors would like to thank the company *Fives Keods* for their financial support.

Appendix A. Numerical algorithm

The mixed-mode model is implemented for the cementite-ferrite to austenite transformation based on Mecozzi et al.'s method [21]. The problem is solved with an explicit finite-difference approach and sharp austenite/ferrite interface as schematically shown in Fig. A1. The green and blue meshing respectively represent the concentration profiles at time t and $t + dt$. In between these two time steps, the interface has advanced of $dz^* = v dt$. The following nomenclature was established: classes are noted i , the interfacial class is noted i^* , phases (γ or α) are noted j , special grid length is noted δz^j . A step-by-step procedure is developed to combine diffusion-controlled model with interface mobility.

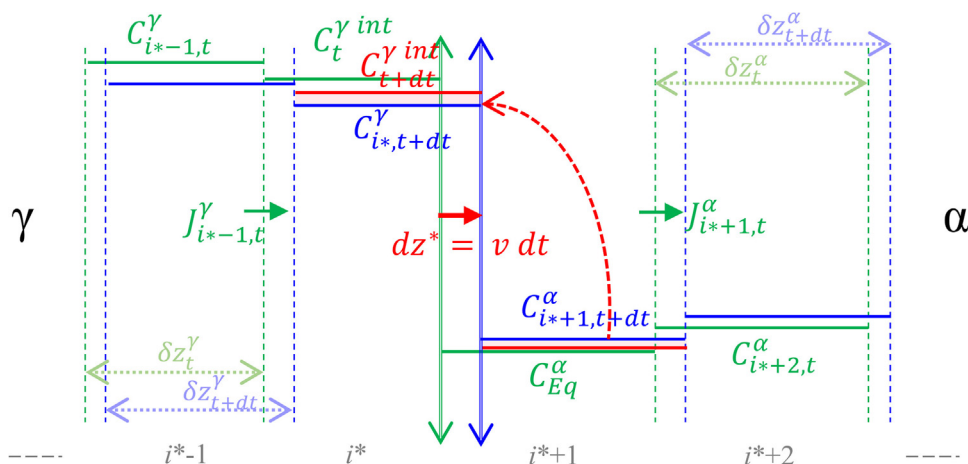


Fig. A1. Schematic representation of the integration scheme for the austenite formation using the mixed-mode model. The green and blue meshing respectively represent the concentration profiles at time t and $t + dt$.

1. First, diffusion fluxes are calculated at each class i (in ferrite and austenite), except for the interface one (i.e. $J_{i,t}^v = 0$) according to first Fick's equation:

$$J_{i,t}^j = -D^j \frac{C_{i+1,t}^j - C_{i,t}^j}{\delta z_t^j} \quad \forall i \neq i^*$$

with D^j the C diffusion coefficient in the j phase (ferrite or austenite).

2. Concentrations are updated for the next time step $t + dt$ (represented in blue colour in Fig. A1):

$$C_{i,t+dt}^j = C_{i,t}^j + (J_{i-1,t}^j - J_{i,t}^j) \frac{dt}{\delta z_t^j} \quad \forall i$$

3. Calculation of the driving pressure ΔG for the interface mobility:

$$\Delta G = \chi(T)(C_t^{yint} - C_{Eq}^y)$$

4. Calculation of interface velocity v and advancement dz^* :

$$v = M\Delta G \rightarrow dz^* = vdt$$

5. Remeshing of the whole system:

$$C_{i,t+dt}^j = \sum_i \frac{C_{i,t+dt}^j}{\delta z_{t+dt}^j} (\delta z_{i,t}^j \cap \delta z_{i,t+dt}^j) \forall i$$

6. The austenite interface composition C_{t+dt}^{yint} is finally adjusted such that the ferrite concentration at the interface equals the equilibrium one (C_{Eq}^x):

$$\begin{cases} C_{t+dt}^{yint} = C_{t+dt}^{yint} + (C_{i^*+1,t+dt}^x - C_{Eq}^x) \frac{\delta z^x}{\delta z^y} \\ C_{i^*+1,t+dt}^x = C_{Eq}^x \end{cases}$$

This latter stage is represented in red colour in Fig. A1. Time is then incremented and the loop is repeated until equilibrium is reached.

References

- [1] S.M.C. van Bohemen, J. Sietsma, *Mat. Sci. Eng.* 527 (24–25) (2010) 6672–6676.
- [2] G.R. Speich, V.A. Demarest, R.L. Miller, *Metall. Trans. A* 12 (8) (1981) 1419–1428.

- [3] J. Huang, W.J. Poole, M. Militzer, *Metall. Mater. Trans. A* 35 (2004) 3363–3375.
- [4] M. Kulakov, W.J. Poole, M. Militzer, *Metall. Mater. Trans. A* 44 (8) (2013) 3564–3576.
- [5] M. Gouné, F. Danoix, J. Ågren, Y. Bréchet, C.R. Hutchinson, M. Militzer, G. Purdy, S. van der Zwaag, H. Zurob, *Mater. Sci. Eng.* 92 (2015) 1–38.
- [6] M. Avrami, *J. Chem. Phys.* 7 (1939) 1103.
- [7] W.A. Johnson, R.F. Mehl, *Trans. Am. Inst. Min. Metall. Pet. Eng.* 135 (1939) 416.
- [8] A. Kolmogorov, *Izv. Acad. Sci. USSR, Math. Ser.* 1 (1937) 355.
- [9] M. Kulakov, W.J. Poole, M. Militzer, *ISIJ Inter.* 54 (11) (2014) 2627–2636.
- [10] M. Ollat, V. Massardier, D. Fabrègue, E. Buscarlet, F. Keovilay, M. Perez, *Metall. Mater. Trans. A* 48 (10) (2017) 4486–4499.
- [11] H. Aaronson, *Inst. Metal.* 47. (1956).
- [12] G.R. Purdy, J.S. Kirkaldy, *Metall. Trans.* 2 (1971) 371–378.
- [13] C. Atkinson, T. Akbay, R.C. Reed, *Acta Metall.* 43 (1995) 2013.
- [14] P.A. Wycliffé, G.R. Purdy, J.D. Embury, *C. Met. Qu.* 20 (1981) 339–350.
- [15] Q. Lai, M. Gouné, A. Pierlade, T. Pardoën, P. Jacques, O. Bouaziz, Y. Bréchet, *Metall. Mater. Trans. A* 47 (7) (2016) 3375–3386.
- [16] J. Christian, Pergamon, (1981).
- [17] G. Purdy, J. Ågren, A. Borgenstam, Y. Bréchet, M. Enomoto, T. Furuhashi, E. Gamsjäger, M. Gouné, M. Hillert, C. Hutchinson, M. Militzer, H. Zurob, *Metall. Mater. Trans.* 42A (2011) 3703–3718.
- [18] J. Sietsma, S. van der Zwaag, *Acta Mater.* 52 (2004) 4143–4152.
- [19] C. Bos, J. Sietsma, *Scripta Mater.* 57 (2007) 1085–1088.
- [20] C. Bos, J. Sietsma, *Acta Mater.* 57 (2009) 136–144.
- [21] M.G. Mecozzi, C. Bos, J. Sietsma, *Acta Mater.* 88 (2015) 302–313.
- [22] H. Chen, S. Zwaag, *Acta Mat.* 72 (2014) 1–12.
- [23] C. Bos, M.G. Mecozzi, J. Sietsma, *Comp. Mater. Sci.* 48 (2009) 692–699.
- [24] J. Rudnizki, B. Bottger, U. Prahl, W. Bleck, *Metall. Mater. Trans. A* 42 (2011) 2516–2525.
- [25] C. Zheng, D. Raabe, *Acta Mater.* 61 (2013) 5504–5517.
- [26] B. Zhu, M. Militzer, *Metall. Mater. Trans. A* 46 (2015) 1073–1084.
- [27] C. Qiu, H. Zurob, C. Hutchinson, *Acta Mater.* 100 (2015) 333–343.
- [28] H.P. van Landeghem, B. Langelier, B. Gault, D. Panahi, A. Korinek, G.R. Purdy, H. S. Zurob, *Acta Mater.* 124 (2017) 536–543.
- [29] J.O. Andersson, T. Helander, L. Hoglund, P.F. Shi, B. Sundman, *Comp. Tools Mater. Sci. Calphad* 26 (2002) 273–312.
- [30] Thermo-Calc software TCFE8 Steels/Fe-alloys database version 8 (accessed 23.07.16).
- [31] M. Gouné, P. Maudis, J. Drillet, *J. Mater. Sci. Technol.* 28 (8) (2012) 728–736.
- [32] H. Bhadeshia, R. Honeycombe, *Steels: Microstructure and properties*, Butterworth-Heinemann, 2006.
- [33] H. Chen, B. Zhu, M. Militzer, *Metall. Mater. Trans.* 88 (2016) 302–313.
- [34] J. Zhu, H. Luo, Z. Yang, C. Zhang, S. van der Zwaag, H. Chen, *Acta Mater.* 133 (2017) 258–268.
- [35] R. Wei, M. Enomoto, R. Hadian, H.S. Zurob, G.R. Purdy, *Acta Mater.* 61 (2013) 697–707.